

1 **Densely sampled viral trajectories for SARS-CoV-2 variants alpha (B.1.1.7) and epsilon**
2 **(B.1.429)**

3
4 Stephen M. Kissler*¹, Joseph R. Fauver*², Christina Mack*^{3,4}, Caroline G. Tai³, Mallery I.
5 Breban², Anne E. Watkins², Radhika M. Samant³, Deverick J. Anderson⁵, David D. Ho⁶, Jessica
6 Metti⁷, Gaurav Khullar⁷, Rachel Baits⁷, Matthew MacKay⁷, Daisy Salgado⁷, Tim Baker⁷, Joel T.
7 Dudley⁷, Christopher E. Mason⁷, Nathan D. Grubaugh^{†2}, Yonatan H. Grad^{†1}

8
9 ¹ Department of Immunology and Infectious Diseases, Harvard T.H. Chan School of Public
10 Health, Boston, MA

11 ² Department of Epidemiology of Microbial Diseases, Yale School of Public Health, New Haven,
12 CT

13 ³ IQVIA, Real World Solutions, Durham, NC

14 ⁴ Department of Epidemiology, University of North Carolina-Chapel Hill, Chapel Hill, NC

15 ⁵ Duke Center for Antimicrobial Stewardship and Infection Prevention, Durham, NC

16 ⁶ Aaron Diamond AIDS Research Center, Columbia University Vagelos College of Physicians
17 and Surgeons, New York, NY

18 ⁷ TEMPUS, Chicago, IL

19
20
21 * denotes equal contribution

22 † denotes co-senior authorship

23
24 Correspondence and requests for materials should be addressed to:

25 Email: ygrad@hsph.harvard.edu

26 Telephone: 617.432.2275

27 **Abstract.**

28

29 We estimated (1) the time from first detectable virus to peak viral concentration (proliferation time),
30 (2) the time from peak viral concentration to initial return to the limit of detection (clearance time),
31 and (3) the peak viral concentration separately for 69 individuals infected with SARS-CoV-2 vari-
32 ants alpha (n=14), epsilon (n=10), and non-variants of interest/variants of concern (VOI/VOCs)
33 (n=45). For individuals infected with alpha, the mean duration of the proliferation phase was 4.3
34 days (95% credible interval [3.0, 6.0]), the mean duration of the clearance phase was 7.4 days
35 [6.0, 9.0], and the mean overall duration of infection (proliferation plus clearance) was 11.7 days
36 [9.8, 13.8]. For individuals infected with epsilon, the mean duration of the proliferation phase was
37 5.6 days [4.0, 7.4], the mean duration of the clearance phase was 8.6 days [6.7, 10.6], and the
38 mean overall duration of infection was 14.2 days [11.8, 16.7]. These compare to a mean prolifer-
39 ation phase of 4.3 days [3.4, 5.4], a mean clearance phase of 6.9 days [6.0, 7.9], and a mean
40 duration of infection of 11.3 days [10.1, 12.5] for non-VOI/VOC infections. The peak viral concen-
41 tration was 20.9 Ct [18.3, 23.5] for alpha, 20.6 Ct [17.8, 23.5] for epsilon, and 20.8 Ct [19.1, 22.4]
42 for VOI/VOCs. This converts to 7.9 log₁₀ RNA copies/ml [7.2, 8.7] for alpha, 8.0 log₁₀ RNA cop-
43 ies/ml [7.2, 8.8] for epsilon, and 8.0 log₁₀ RNA copies/ml [7.5, 8.4] for non-VOI/VOCs. The distri-
44 butions of individual-level means are suggestive of longer clearance times for the VOCs. The
45 overall durations of acute infection varied widely across individuals, with individual posterior mean
46 acute infection durations ranging from 5.5 - 16.1 days for alpha, 9.4 - 20.3 days for epsilon, and
47 4.8 - 17.6 days for non-VOI/VOCs. These data offer evidence that infections with SARS-CoV-2
48 variants alpha and epsilon feature broadly similar viral trajectories as infections with non-
49 VOI/VOCs.

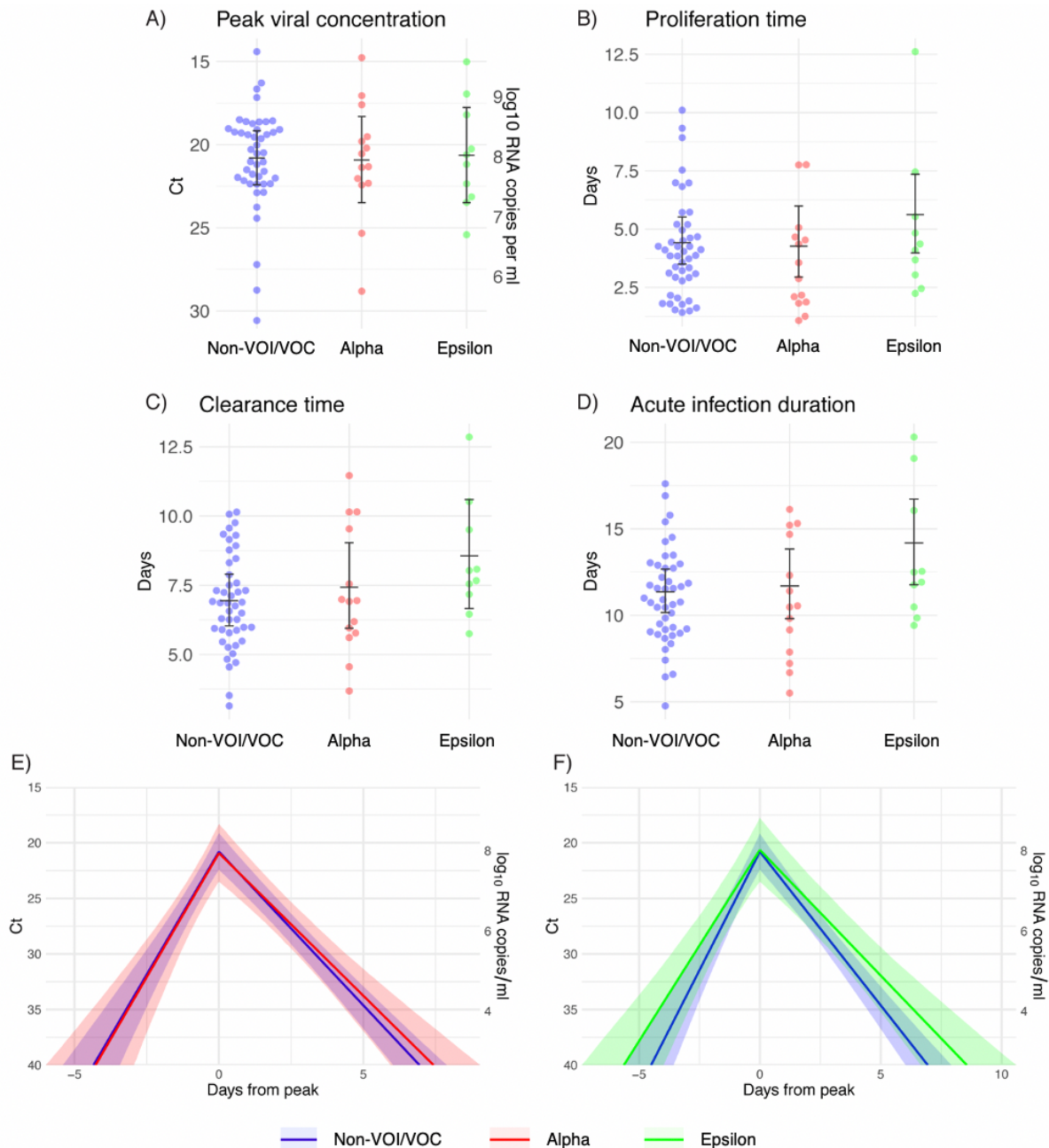
50 **Main text.**

51 The reasons for the enhanced transmissibility of SARS-CoV-2 variants of concern (VOCs)¹ are
52 unclear. Of special interest are the VOCs B.1.1.7 (alpha) and B.1.429 (epsilon), which until April
53 2021 were the most prevalent VOCs in the United States.¹ Variant alpha features multiple muta-
54 tions in the spike protein receptor binding domain² that may enhance ACE-2 binding,³ thus in-
55 creasing the efficiency of virus transmission. Variant epsilon partially evades neutralization by
56 sera from convalescent patients and vaccine recipients.⁴ In addition to, and perhaps due to, these
57 attributes, the viral trajectories for infections with alpha or epsilon could feature a higher peak viral
58 load or longer duration of carriage, both of which could increase transmissibility. To test whether
59 acute infections with SARS-CoV-2 VOCs alpha or epsilon are associated with higher or more
60 sustained nasopharyngeal viral concentrations relative to non-variants of interest and non-vari-
61 ants of concern (non-VOI/VOCs), we assessed longitudinal densely sampled PCR tests per-
62 formed in a cohort of 69 individuals (**Supplementary Table 1**) infected with SARS-CoV-2 under-
63 going daily surveillance testing, including 14 infected with alpha and 10 infected with epsilon, with
64 lineage assignments confirmed by whole genome sequencing.

65
66 We estimated (1) the time from first detectable virus to peak viral concentration (proliferation time),
67 (2) the time from peak viral concentration to initial return to the limit of detection (clearance time),
68 and (3) the peak viral concentration for each individual (**Supplementary Appendix**).⁵ We esti-
69 mated the means of these quantities separately for individuals infected with alpha, epsilon, and
70 non-VOI/VOCs (**Figure 1; Supplementary Table 2**). For individuals infected with alpha, the mean
71 duration of the proliferation phase was 4.3 days (95% credible interval [3.0, 6.0]), the mean dura-
72 tion of the clearance phase was 7.4 days [6.0, 9.0], and the mean overall duration of infection
73 (proliferation plus clearance) was 11.7 days [9.8, 13.8]. For individuals infected with epsilon, the
74 mean duration of the proliferation phase was 5.6 days [4.0, 7.4], the mean duration of the clear-
75 ance phase was 8.6 days [6.7, 10.6], and the mean overall duration of infection was 14.2 days
76 [11.8, 16.7]. These compare to a mean proliferation phase of 4.3 days [3.4, 5.4], a mean clearance
77 phase of 6.9 days [6.0, 7.9], and a mean duration of infection of 11.3 days [10.1, 12.5] for non-
78 VOI/VOC infections. The peak viral concentration was 20.9 Ct [18.3, 23.5] for alpha, 20.6 Ct [17.8,
79 23.5] for epsilon, and 20.8 Ct [19.1, 22.4] for VOI/VOCs. This converts to 7.9 log₁₀ RNA copies/ml
80 [7.2, 8.7] for alpha, 8.0 log₁₀ RNA copies/ml [7.2, 8.8] for epsilon, and 8.0 log₁₀ RNA copies/ml
81 [7.5, 8.4] for non-VOI/VOCs. We found no evidence of variant-specific differences in the popula-
82 tion means for these parameters, as assessed by overlapping 95% credible intervals, and no

83 differences in empirical distribution, as assessed by a Kolmogorov-Smirnov test⁶ with significance
84 threshold $\alpha = 0.05$. However, the distributions of individual-level means are suggestive of longer
85 clearance times for the VOCs (**Figure 1C**). The overall durations of acute infection varied widely
86 across individuals, with individual posterior mean acute infection durations ranging from 5.5 –
87 16.1 days for alpha, 9.4 – 20.3 days for epsilon, and 4.8 – 17.6 days for non-VOI/VOCs (**Supple-**
88 **mentary Table 3**). Data and code are available online.⁷

89
90 These data offer evidence that infections with SARS-CoV-2 variants alpha and epsilon feature
91 broadly similar viral trajectories as infections with non-VOI/VOCs. Our ability to detect differences
92 in the trajectories was limited by small sample sizes and a high degree of interpersonal variation.
93 The findings should be seen as preliminary, as they are based on fourteen alpha cases and ten
94 epsilon cases. The possibility of an extended clearance time for SARS-CoV-2 VOCs merits further
95 investigation; if borne out by additional data, a longer isolation period than the currently recom-
96 mended 10 days after symptom onset⁸ may be needed to effectively interrupt secondary infec-
97 tions by some VOCs. Collection of longitudinal PCR and test positivity data in larger and more
98 diverse cohorts is urgently needed.



99
100
101
102
103
104
105
106

Figure 1. Estimated viral trajectory parameters for SARS-CoV-2 infections with alpha, epsilon, and non-variants of interest/non-variants of concern. Individual posterior means (points) with population means and 95% credible intervals (hatched lines) for (A) the mean peak viral concentration, (B) the mean proliferation duration, (C) the mean clearance duration, and (D) the mean total duration of acute infection. The points are jittered horizontally to avoid overlap. Solid lines in panels (E)-(F) depict the mean posterior viral trajectories for alpha infections (red) and epsilon infections (green) respectively, relative to non-VOI/VOC infections (blue), as specified by the population means and credible intervals in (A)-(D). The shaded regions represent 95% credible areas for the mean population trajectories.

References

1. Centers for Disease Control and Prevention. COVID Data Tracker. Published 2021. Accessed May 20, 2021. <https://covid.cdc.gov/covid-data-tracker/>
2. Galloway SE, Paul P, MacCannell DR, Johansson MA, Brooks JT, MacNeil A, et al. Emergence of SARS-CoV-2 B.1.1.7 Lineage — United States, December 29, 2020–January 12, 2021. *MMWR Morb Mortal Wkly Rep.* 2021;70(3):95-99. doi:10.15585/mmwr.mm7003e2
3. Yi C, Sun X, Ye J, Ding L, Liu M, Yang Z, et al. Key residues of the receptor binding motif in the spike protein of SARS-CoV-2 that interact with ACE2 and neutralizing antibodies. *Cell Mol Immunol.* 2020;17(6):621-630. doi:10.1038/s41423-020-0458-z
4. Deng X, Garcia-Knight MA, Khalid MM, Servellita V, Wang C, Morris MK, et al. Transmission, infectivity, and antibody neutralization of an emerging SARS-CoV-2 variant in California carrying a L452R spike protein mutation. *medRxiv.* Published online 2021.
5. Kissler SM, Fauver JR, Mack C, Olesen SW, Tai C, Shiue KY, et al. SARS-CoV-2 viral dynamics in acute infections. *medRxiv.* Published online 2020:1-13. doi:10.1101/2020.10.21.20217042
6. Conover WJ. *Practical Nonparametric Statistics.* John Wiley & Sons; 1971.
7. Kissler SM. Github Repository: CtTrajectories_B117. Published 2021. Accessed June 14, 2021. https://github.com/gradlab/CtTrajectories_AllVariants
8. Centers for Disease Control and Prevention. Duration of Isolation and Precautions for Adults with COVID-19. COVID-19. Published 2020. Accessed February 8, 2020. <https://www.cdc.gov/coronavirus/2019-ncov/hcp/duration-isolation.html>
9. United States Food and Drug Administration. *Emergency Use Authorization for TaqPath COVID-19 Combo Kit.*; 2020. <https://www.fda.gov/media/136113/download>
10. Loman N, Rowe W, Rambaut A. nCoV-2019 novel coronavirus bioinformatics protocol.
11. Illumina. *Illumina COVIDSeq Test Instructions for Use.*; 2021. <https://www.fda.gov/media/138776/download>
12. Illumina. NextSeq 550 System Documentation. Published 2021. Accessed June 10, 2021. https://support.illumina.com/sequencing/sequencing_instruments/nextseq-550/documentation.html
13. BaseSpace Labs. DRAGEN COVID Lineage. Published online 2021.
14. Rambaut A, Holmes EC, O’Toole Á, Hill V, McCrone JT, Ruis C, et al. A dynamic nomenclature proposal for SARS-CoV-2 lineages to assist genomic epidemiology. *Nat Microbiol.* 2020;5(11):1403-1407. doi:10.1038/s41564-020-0770-5
15. Aksamentov I, Neher R. NextClade. Published 2021. Accessed June 10, 2021. <https://clades.nextstrain.org/>
16. Kudo E, Israelow B, Vogels CBF, Lu P, Wyllie AL, Tokuyama M, et al. Detection of SARS-CoV-2 RNA by multiplex RT-qPCR. Sugden B, ed. *PLOS Biol.* 2020;18(10):e3000867. doi:10.1371/journal.pbio.3000867
17. Vogels C, Fauver J, Ott IM, Grubaugh N. *Generation of SARS-COV-2 RNA Transcript Standards for QRT-PCR Detection Assays.*; 2020. doi:10.17504/protocols.io.bdv6i69e
18. Cleary B, Hay JA, Blumenstiel B, Gabriel S, Regev A, Mina MJ. Efficient prevalence estimation and infected sample identification with group testing for SARS-CoV-2. *medRxiv.* Published online 2020.
19. Tom MR, Mina MJ. To Interpret the SARS-CoV-2 Test, Consider the Cycle Threshold Value. *Clin Infect Dis.* 2020;02115(Xx):1-3. doi:10.1093/cid/ciaa619
20. Carpenter B, Gelman A, Hoffman MD, Lee D, Goodrich B, Betancourt M, et al. Stan : A Probabilistic Programming Language. *J Stat Softw.* 2017;76(1). doi:10.18637/jss.v076.i01

- 156 21. R Development Core Team R. R: A Language and Environment for Statistical Computing.
157 Team RDC, ed. *R Found Stat Comput.* 2011;1(2.11.1):409. doi:10.1007/978-3-540-
158 74686-7
159

160 **Supplementary Appendix.**

161
162 Ethics.

163 Residual de-identified viral transport media from anterior nares and oropharyngeal swabs
164 collected from players, staff, vendors, and associated household members from a professional
165 sports league were obtained from BioReference Laboratories. In accordance with the guidelines
166 of the Yale Human Investigations Committee, this work with de-identified samples was approved
167 for research not involving human subjects by the Yale Internal Review Board (HIC protocol #
168 2000028599). This project was designated exempt by the Harvard IRB (IRB20-1407).

169
170 Study population. The data reported here represent a convenience sample including team staff,
171 players, arena staff, and other vendors (e.g., transportation, facilities maintenance, and food
172 preparation) affiliated with a professional sports league. Clinical samples were obtained by
173 combined swabs of the anterior nares and oropharynx administered by a trained provider. Viral
174 concentration was measured using the cycle threshold (Ct) according to the Roche cobas target
175 1 assay. For an initial pool of 589 participants who first tested positive for SARS-CoV-2 infection
176 during the study period (between November 28th, 2020 and May 4th, 2021), a diagnosis of “novel”
177 or “persistent” infection was recorded. “Novel” denoted a likely new infection while “persistent”
178 indicated the presence of virus in a clinically recovered individual. A total of 69 individuals (90%
179 male) had novel infections that met our inclusion criteria: at least five positive PCR tests (Ct < 40),
180 at least one negative PCR test (Ct = 40), at least one test with Ct < 32, and a genetic lineage of
181 either B.1.1.7, B.1.429, or non-variant of interest/non-variant of concern (that is, we excluded
182 lineages B.1.427, P.1, B.1.351, B.1.526, B.1.526.1, B.1.526.2, and P.2, of which there were 8
183 infections in total) as confirmed by whole genome sequencing. Fourteen of the individuals who
184 met the inclusion criteria were infected with B.1.1.7 (alpha) and ten were infected with B.1.429
185 (epsilon).

186
187 Genome sequencing and lineage assignments

188 RNA was extracted and confirmed as SARS-CoV-2 positive by RT-qPCR with the Thermo Fisher
189 TaqPath SARS-CoV-2 assay.⁹ Next Generation Sequencing with the Illumina COVIDSeq ARTIC
190 primer set¹⁰ was used for viral amplification. Library preparation was performed using the am-
191 plicon-based Illumina COVIDseq Test v03¹¹ and sequenced 2x74 on Illumina NextSeq 550 fol-
192 lowing the protocol as described in Illumina's documentation.¹² The resulting FASTQs were

193 processed and analyzed on Illumina BaseSpace Labs using the Illumina DRAGEN COVID Line-
194 age Application;¹³ versions included are 3.5.0, 3.5.1, 3.5.2, and 3.5.3. The DRAGEN COVID Lin-
195 eage pipeline was run with default parameters recommended by Illumina. Samples were consid-
196 ered SARS-COV-2 positive if at least 5 viral amplicon targets were detected at 20x coverage.
197 Each SARS-COV-2 positive sample underwent lineage assignment and phylogenetics analysis
198 using the most updated version of Pangolin¹⁴ and NextClade,¹⁵ respectively.

199
200 Converting Ct values to viral genome equivalents. To convert Ct values to viral genome
201 equivalents, we first converted the Roche cobas target 1 Ct values to equivalent Ct values on a
202 multiplexed version of the RT-qPCR assay from the US Centers for Disease Control and
203 Prevention.¹⁶ We did this following our previously described methods.⁵ Briefly, we adjusted the
204 Ct values using the best-fit linear regression between previously collected Roche cobas target 1
205 Ct values and CDC multiplex Ct values using the following regression equation:

$$y_i = \beta_0 + \beta_1 x_i + \epsilon_i \quad (\text{S1})$$

206
207 Here, y_i denotes the i^{th} Ct value from the CDC multiplex assay, x_i denotes the i^{th} Ct value from the
208 Roche cobas target 1 test, and ϵ_i is an error term with mean 0 and constant variance across all
209 samples. The coefficient values are $\beta_0 = -6.25$ and $\beta_1 = 1.34$.

210
211
212
213 Ct values were fitted to a standard curve in order to convert Ct value data to RNA copies. Synthetic
214 T7 RNA transcripts corresponding to a 1,363 b.p. segment of the SARS-CoV-2 nucleocapsid gene
215 were serially diluted from 10^6 - 10^0 RNA copies/ μl in duplicate to generate a standard curve¹⁷
216 **(Supplementary Table 4)**. The average Ct value for each dilution was used to calculate the slope
217 (-3.60971) and intercept (40.93733) of the linear regression of Ct on log-10 transformed standard
218 RNA concentration, and Ct values from subsequent RT-qPCR runs were converted to RNA copies
219 using the following equation:

$$\log_{10}([\text{RNA}]) = (Ct - 40.93733)/(-3.60971) + \log_{10}(250) \quad (\text{S2})$$

220
221
222
223 Here, [RNA] represents the RNA copies /ml. The $\log_{10}(250)$ term accounts for the extraction (300
224 μl) and elution (75 μl) volumes associated with processing the clinical samples as well as the
225 1,000 $\mu\text{l}/\text{ml}$ unit conversion.

226

227 Model fitting.

228 For the statistical analysis, we removed any sequences of 3 or more consecutive negative tests
229 to avoid overfitting to these trivial values. Following our previously described methods,⁵ we
230 assumed that the viral concentration trajectories consisted of a proliferation phase, with
231 exponential growth in viral RNA concentration, followed by a clearance phase characterized by
232 exponential decay in viral RNA concentration.¹⁸ Since Ct values are roughly proportional to the
233 negative logarithm of viral concentration¹⁹, this corresponds to a linear decrease in Ct followed by
234 a linear increase. We therefore constructed a piecewise-linear regression model to estimate the
235 peak Ct value, the time from infection onset to peak (*i.e.* the duration of the proliferation stage),
236 and the time from peak to infection resolution (*i.e.* the duration of the clearance stage). The
237 trajectory may be represented by the equation

238

$$E[Ct(t)] = \begin{cases} \text{l.o.d.} & t \leq t_o \\ \text{l.o.d.} - \frac{\delta}{t_p - t_o}(t - t_o) & t_o < t \leq t_p \\ \text{l.o.d.} - \delta + \frac{\delta}{t_r - t_p}(t - t_p) & t_p < t \leq t_r \\ \text{l.o.d.} & t > t_r \end{cases} \quad (\text{S3})$$

239

240

241 Here, $E[Ct(t)]$ represents the expected value of the Ct at time t , “l.o.d” represents the RT-qPCR
242 limit of detection, δ is the absolute difference in Ct between the limit of detection and the peak
243 (lowest) Ct, and t_o , t_p , and t_r are the onset, peak, and recovery times, respectively.

244

245 Before fitting, we re-parametrized the model using the following definitions:

246

- 247 • $\Delta Ct(t) = \text{l.o.d.} - Ct(t)$ is the difference between the limit of detection and the observed Ct
248 value at time t .
- 249 • $\omega_p = t_p - t_o$ is the duration of the proliferation stage.
- 250 • $\omega_r = t_r - t_p$ is the duration of the clearance stage.

251

252 We constrained $0.25 \leq \omega_p \leq 14$ days and $2 \leq \omega_r \leq 30$ days to prevent inferring unrealistically small
253 or large values for these parameters for trajectories that were missing data prior to the peak and

254 after the peak, respectively. We also constrained $0 \leq \delta \leq 40$ as Ct values can only take values
255 between 0 and the limit of detection (40).

256

257 We next assumed that the observed $\Delta Ct(t)$ could be described the following mixture model:

258

$$259 \quad \Delta Ct(t) \sim \lambda \text{Normal}(E[\Delta Ct(t)], \sigma(t)) + (1 - \lambda) \text{Exponential}(\log(10)) \Big]_0^{\text{l.o.d}} \quad (\text{S4})$$

260

261 where $E[\Delta Ct(t)] = \text{l.o.d.} - E[Ct(t)]$ and λ is the sensitivity of the q-PCR test, which we fixed at 0.99.
262 The bracket term on the right-hand side of the equation denotes that the distribution was truncated
263 to ensure Ct values between 0 and the limit of detection. This model captures the scenario where
264 most observed Ct values are normally distributed around the expected trajectory with standard
265 deviation $\sigma(t)$, yet there is a small (1%) probability of an exponentially distributed false negative
266 near the limit of detection. The $\log(10)$ rate of the exponential distribution was chosen so that 90%
267 of the mass of the distribution sat below 1 Ct unit and 99% of the distribution sat below 2 Ct units,
268 ensuring that the distribution captures values distributed at or near the limit of detection. We did
269 not estimate values for λ or the exponential rate because they were not of interest in this study;
270 we simply needed to include them to account for some small probability mass that persisted near
271 the limit of detection to allow for the possibility of false negatives.

272

273 We used a hierarchical structure to describe the distributions of ω_p , ω_r , and δ for each individual
274 based on their respective population means μ_{ω_p} , μ_{ω_r} , and μ_{δ} and population standard deviations
275 σ_{ω_p} , σ_{ω_r} , and σ_{δ} such that

276

$$277 \quad \omega_p \sim \text{Normal}(\mu_{\omega_p}, \sigma_{\omega_p}) \quad (\text{S5})$$

$$278 \quad \omega_r \sim \text{Normal}(\mu_{\omega_r}, \sigma_{\omega_r})$$

$$279 \quad \delta \sim \text{Normal}(\mu_{\delta}, \sigma_{\delta})$$

280

281 We inferred population means (μ) separately for individuals infected with alpha, epsilon, and non-
282 VOI/VOCs. We used a Hamiltonian Monte Carlo fitting procedure implemented in Stan (version
283 2.24)²⁰ and R (version 3.6.2)²¹ to estimate the individual-level parameters ω_p , ω_r , δ , and t_p as well
284 as the population-level parameters σ^* , μ_{ω_p} , μ_{ω_r} , μ_{δ} , σ_{ω_p} , σ_{ω_r} , and σ_{δ} . We used the following priors:

285

286 *Hyperparameters:*

287

$$288 \sigma^* \sim \text{Cauchy}(0, 5) [0, \infty] \quad (\text{S6})$$

289

$$290 \mu_{\omega p} \sim \text{Normal}(14/2, 14/6) [0.25, 14] \quad (\text{S7})$$

$$291 \mu_{\omega r} \sim \text{Normal}(30/2, 30/6) [2, 30]$$

$$292 \mu_{\delta} \sim \text{Normal}(40/2, 40/6) [0, 40]$$

293

$$294 \sigma_{\omega p} \sim \text{Cauchy}(0, 14/\tan(\pi(0.95-0.5))) [0, \infty] \quad (\text{S8})$$

$$295 \sigma_{\omega r} \sim \text{Cauchy}(0, 30/\tan(\pi(0.95-0.5))) [0, \infty]$$

$$296 \sigma_{\delta} \sim \text{Cauchy}(0, 40/\tan(\pi(0.95-0.5))) [0, \infty]$$

297

298 *Individual-level parameters:*

$$299 \omega_p \sim \text{Normal}(\mu_{\omega p}, \sigma_{\omega p}) [0.25, 14]$$

$$300 \omega_r \sim \text{Normal}(\mu_{\omega r}, \sigma_{\omega r}) [2, 30] \quad (\text{S9})$$

$$301 \delta \sim \text{Normal}(\mu_{\delta}, \sigma_{\delta}) [0, 40]$$

$$302 t_p \sim \text{Normal}(0, 2)$$

303

304 The values in square brackets denote truncation bounds for the distributions. We chose a vague
305 half-Cauchy prior with scale 5 for the observation variance σ^* . The priors for the population mean
306 values (μ_{\cdot}) are normally distributed priors spanning the range of allowable values for that
307 parameter; this prior is vague but expresses a mild preference for values near the center of the
308 allowable range. The priors for the population standard deviations (σ_{\cdot}) are half Cauchy-distributed
309 with scale chosen so that 90% of the distribution sits below the maximum value for that parameter;
310 this prior is vague but expresses a mild preference for standard deviations close to 0.

311

312 We ran four MCMC chains for 1,000 iterations each with a target average proposal acceptance
313 probability of 0.8. The first half of each chain was discarded as the warm-up. The Gelman R-hat
314 statistic was less than 1.1 for all parameters. This indicates good overall mixing of the chains.
315 There were no divergent iterations, indicating good exploration of the parameter space. The
316 posterior distributions for μ_{δ} , $\mu_{\omega p}$, and $\mu_{\omega r}$, were estimated separately for individuals infected with
317 alpha, epsilon, and non-VOI/VOCs. These are depicted in **Figure 1** (main text). Draws from the

318 individual posterior viral trajectory distributions are depicted in **Supplementary Figures 1-2**. The
319 mean posterior viral trajectories for each individual are depicted in **Supplementary Figure 3**.

320

321 Assessing sensitivity to different priors.

322 To ensure that our findings were not overly influenced by the prior distributions, we re-fit the model
323 using two different sets of priors. The first set used the posterior population means from a previous
324 study in a similar population as the prior values for $\mu_{\omega p}$, $\mu_{\omega r}$, and μ_{δ} . These priors were defined
325 by

326

$$\begin{aligned} 327 \mu_{\omega p} &\sim \text{Normal}(2.7, 14/6) [0.25, 14] \\ 328 \mu_{\omega r} &\sim \text{Normal}(7.4, 30/6) [2, 30] \\ 329 \mu_{\delta} &\sim \text{Normal}(20, 40/6) [0, 40]. \end{aligned} \tag{S10}$$

330

331 The second set used unrealistically low prior means for $\mu_{\omega p}$, $\mu_{\omega r}$, and μ_{δ} to verify that the
332 suggestion of longer clearance times for alpha and epsilon infections was informed by the data
333 and not solely by a biased prior distribution. These priors were defined by

334

$$\begin{aligned} 335 \mu_{\omega p} &\sim \text{Normal}(0, 14/6) [0.25, 14] \\ 336 \mu_{\omega r} &\sim \text{Normal}(0, 30/6) [2, 30] \\ 337 \mu_{\delta} &\sim \text{Normal}(20, 40/6) [0, 40]. \end{aligned} \tag{S11}$$

338

339 Note that we updated the prior means but kept the prior variances at their original wide values to
340 avoid encoding over-confidence in the priors into the model. The posterior population means for
341 these new sets of priors are depicted in **Supplementary Figures 4-5** (compare to **Figure 1**).

342 Overall, the findings were consistent across choices of prior.

	Alpha (%)	Epsilon (%)	Non-VOI/VOC (%)	Total (%)
Total	14 (20)	10 (14)	45 (65)	69 (100)
Age				
<18	0 (0)	0 (0)	0 (0)	0 (0)
18-29	12 (17)	4 (6)	26 (38)	42 (61)
30-39	2 (3)	3 (4)	9 (13)	14 (20)
40-49	0 (0)	2 (3)	3 (4)	5 (7)
50-59	0 (0)	1 (1)	4 (6)	5 (7)
≥60				3 (4)
Symptoms reported				
Yes	6 (9)	5 (7)	17 (25)	28 (41)
No	8 (12)	5 (7)	28 (41)	41 (59)

344 **Supplementary Table 1. Characteristics of the study population.** Number and percent (in parentheses) of
345 individuals in the study population by age group and reported symptoms, stratified by variant.
346

	Minimum Ct	Maximum viral concentration (log ₁₀ RNA copies/ml)	Proliferation duration (days)	Clearance duration (days)	Acute infection duration (days)
Alpha	20.92 [18.31, 23.49]	7.94 [7.23, 8.67]	4.27 [2.95, 5.99]	7.43 [5.95, 9.03]	11.7 [9.80, 13.84]
Epsilon	20.64 [17.76, 23.49]	8.02 [7.23, 8.82]	5.62 [3.98, 7.36]	8.56 [6.66, 10.60]	14.19 [11.76, 16.71]
Non-VOI/VOIC	20.80 [19.14, 22.42]	7.98 [7.53, 8.44]	4.34 [3.43, 5.39]	6.94 [6.03, 7.89]	11.28 [10.11, 12.54]

347
348
349
350
351

Supplementary Table 2. Posterior population viral trajectory parameters for SARS-CoV-2 infections with alpha, epsilon, and non-variants of interest/variants of concern. Reported values represent the posterior mean and 95% credible intervals (brackets) for each parameter.

	Minimum Ct	Maximum viral concentration (log ₁₀ RNA copies/ml)	Proliferation duration (days)	Clearance duration (days)	Acute infection duration (days)
Alpha					
Median	20.9	7.94	3.22	6.93	10.5
IQR	[19.6, 22.2]	[7.58, 8.31]	[1.93, 4.63]	[5.82, 9.04]	[8.19, 14.1]
Range	[14.8, 28.8]	[5.76, 9.65]	[1.08, 7.76]	[3.68, 11.5]	[5.50, 16.1]
Epsilon					
Median	20.9	7.95	4.23	7.85	12.2
IQR	[18.7, 22.9]	[7.38, 8.55]	[3.20, 5.36]	[7.27, 9.15]	[10.80, 15.2]
Range	[15.0, 25.4]	[6.70, 9.58]	[2.24, 12.60]	[5.75, 12.9]	[9.42, 20.3]
Non-VOI/VOC					
Median	20.5	8.06	3.87	6.86	10.9
IQR	[19.1, 22.2]	[7.60, 8.45]	[2.92, 4.96]	[5.87, 7.88]	[9.17, 12.7]
Range	[14.4, 30.6]	[5.27, 9.75]	[1.42, 10.10]	[3.14, 10.1]	[4.77, 17.6]

352

353

354

355

356

357

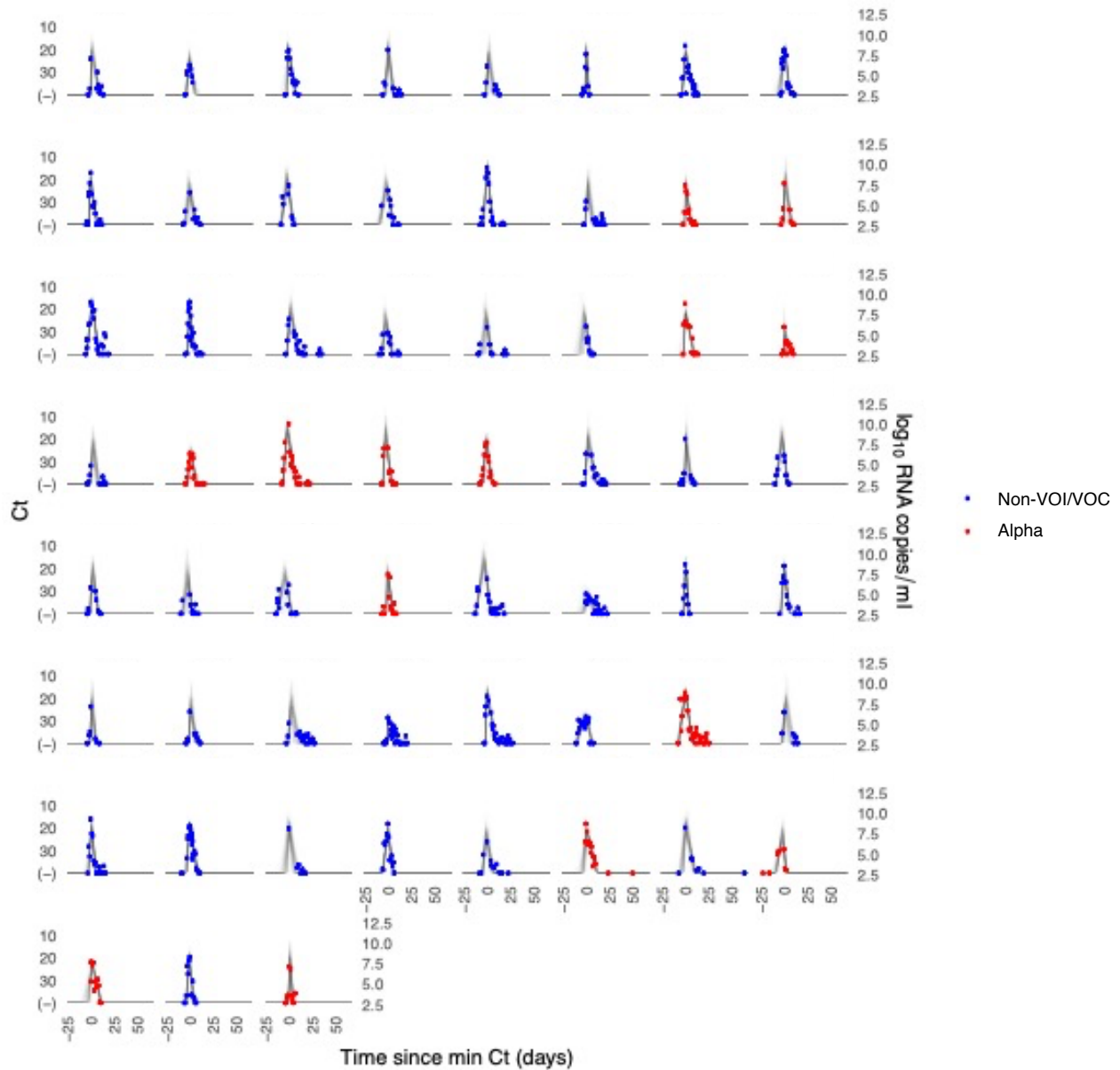
Supplementary Table 3. Summary of individual-level viral trajectory parameter means for SARS-CoV-2 infections with alpha, epsilon, and non-variants of interest/variants of concern. Reported values represent the median, inner quartile range, and full range of individual-level posterior means for each parameter.

Standard (copies/ul)	Replicate 1 (Ct)	Replicate 2 (Ct)	Average Ct
10 ⁶	19.3	19.7	19.5
10 ⁵	23.0	21.2	22.1
10 ⁴	26.9	26.7	26.8
10 ³	30.6	30.4	30.5
10 ²	34.0	34.0	34.0
10 ¹	37.2	36.6	36.9
10 ⁰	N/A	39.9	39.9

359

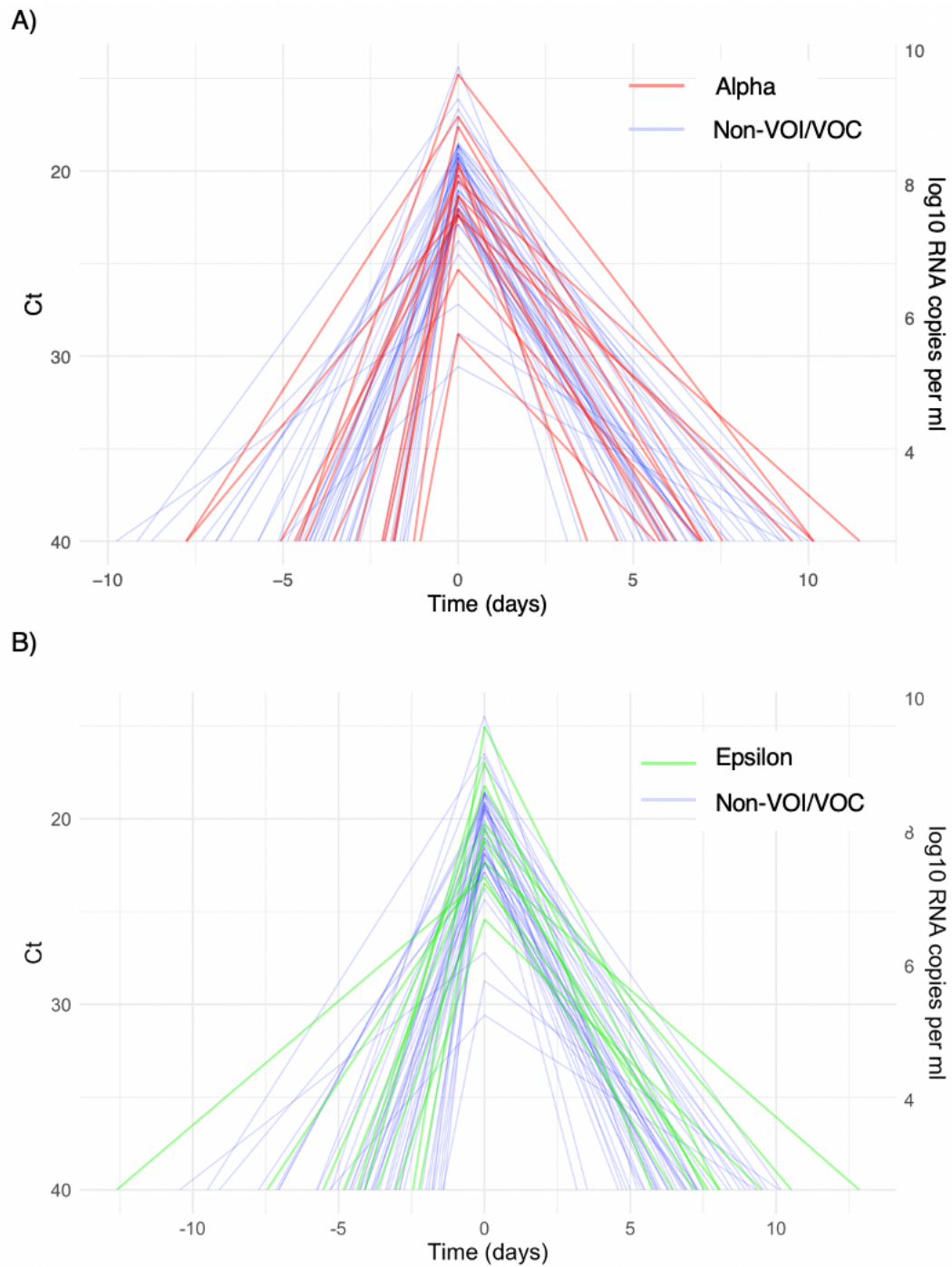
360 **Supplementary Table 4. Standard curve relationship between virus RNA copies and Ct values.** Synthetic T7
361 RNA transcripts corresponding to a 1,363 base pair segment of the SARS-CoV-2 nucleocapsid gene were serially
362 diluted from 10⁶-10⁰ and evaluated in duplicate with RT-qPCR. The best-fit linear regression of the average Ct on the
363 log₁₀-transformed standard values had slope -3.60971 and intercept 40.93733 (R² = 0.99).
364

365
366



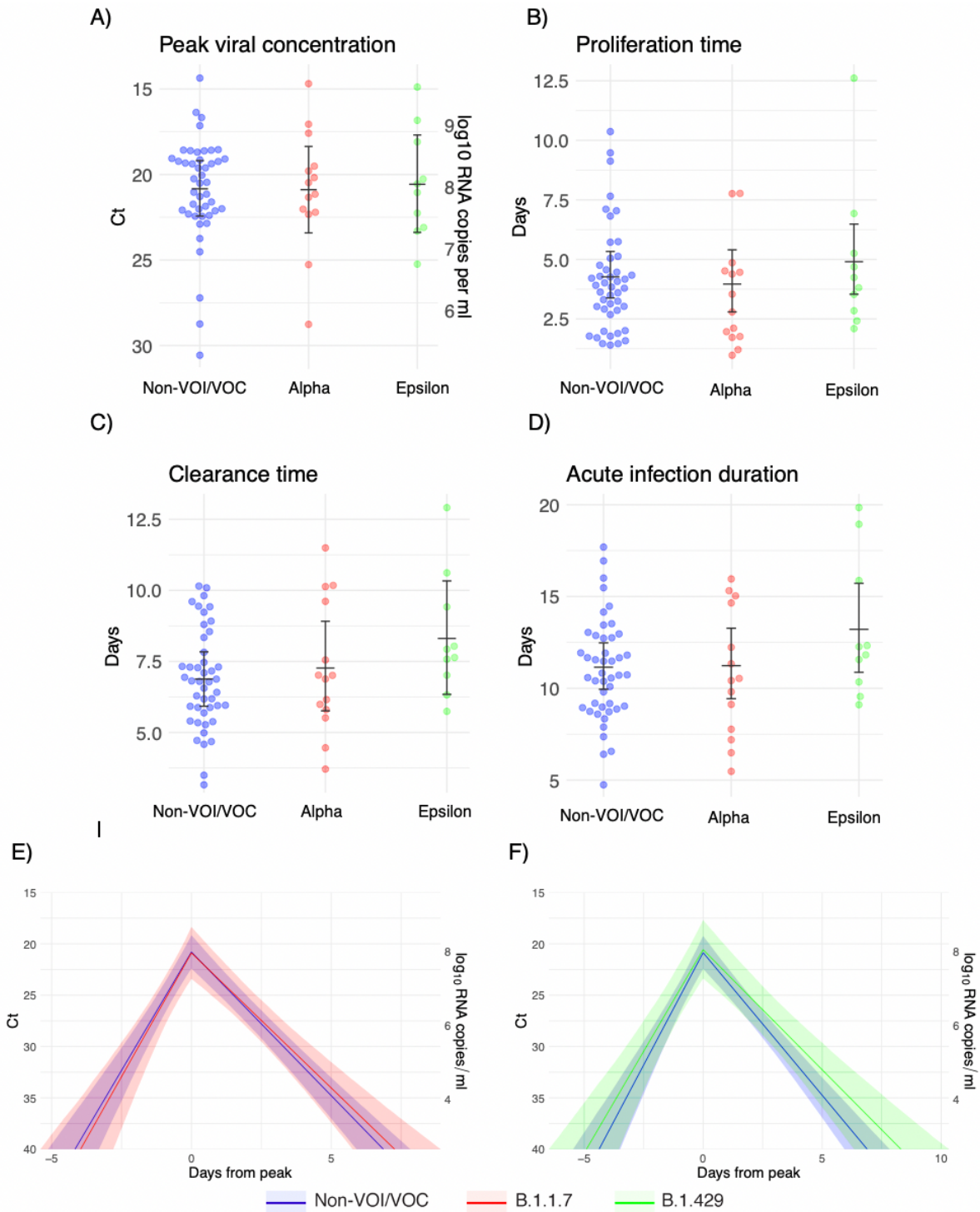
367
368
369
370
371
372
373
374
375

Supplementary Figure 1. Ct values and estimated trajectories for alpha variant and non-VOI/VOC SARS-CoV-2 infections. Each pane depicts the recorded Ct values (points) and derived log-10 genome equivalents per ml (log₁₀(ge/ml)) for a single person during the study period. Points along the horizontal axis represent negative tests. Time is indexed in days since the minimum recorded Ct value (maximum viral concentration). Individuals with confirmed alpha infections are depicted in red. Non-VOI/VOC infections are depicted in blue. Lines depict 100 draws from the posterior distribution for each person's viral trajectory.



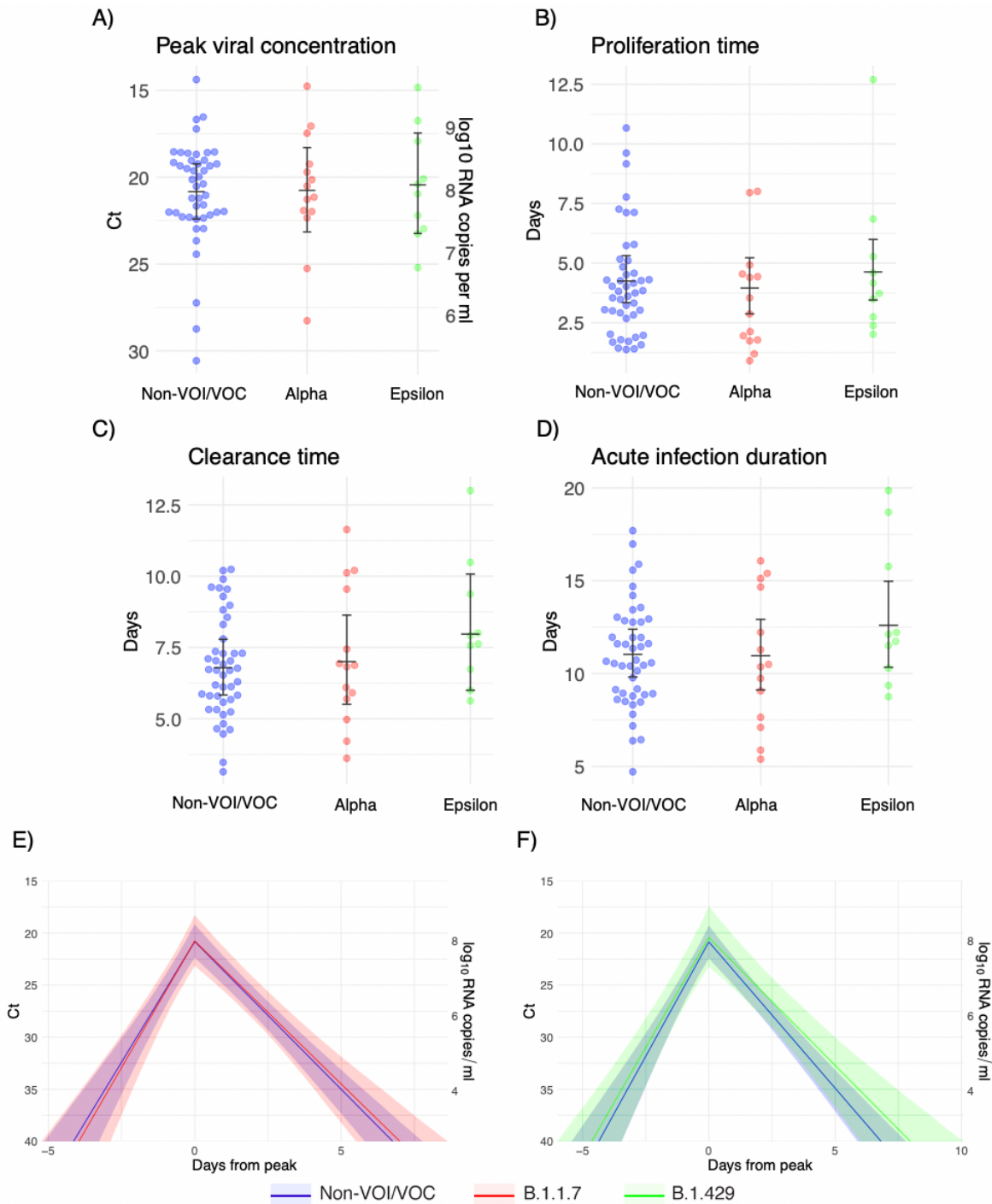
385
 386
 387
 388
 389
 390
 391

Supplementary Figure 3. Mean posterior viral trajectories for each individual. Panel (A) depicts alpha infections (red) against non-VOI/VOC infections (blue). Panel (B) depicts epsilon infections (green) against non-VOI/VOC infections (blue). Trajectories are aligned temporally to have the same peak time.



392
 393
 394
 395
 396
 397
 398
 399
 400

Supplementary Figure 4. Estimated viral trajectory parameters for SARS-CoV-2 infections with alpha, epsilon, and non-variants of interest/non-variants of concern using informative priors. Individual posterior means (points) with population means and 95% credible intervals (hatched lines) for (A) the mean peak viral concentration, (B) the mean proliferation duration, (C) the mean clearance duration, and (D) the mean total duration of acute infection. Points are jittered horizontally to avoid overlap. Solid lines in panels (E)-(F) depict the mean posterior viral trajectories for alpha infections (red) and epsilon infections (green) respectively, relative to non-VOI/VOC infections (blue), as specified by the population means and credible intervals in (A)-(D). The shaded regions represent 95% credible areas for the mean population trajectories. Priors were informed by a previous analysis and are defined in Eq. (S10).



401
 402 **Supplementary Figure 5. Estimated viral trajectory parameters for SARS-CoV-2 infections with alpha, epsilon,**
 403 **and non-variants of interest/non-variants of concern using low priors.** Individual posterior means (points)
 404 with population means and 95% credible intervals (hatched lines) for (A) the mean peak viral concentration,
 405 (B) the mean proliferation duration, (C) the mean clearance duration, and (D) the mean total duration of acute infection.
 406 Points are jittered horizontally to avoid overlap. Solid lines in panels (E)-(F) depict the mean posterior viral trajectories for alpha
 407 infections (red) and epsilon infections (green) respectively, relative to non-VOI/VOC infections (blue), as specified by
 408 the population means and credible intervals in (A)-(D). The shaded regions represent 95% credible areas for the mean
 409 population trajectories. Priors were chosen to be unrealistically low and are defined in Eq. (S11).
 410